Environmental Science and Pollution Research (2022) 29:70269–70284
https://doi.org/10.1007/s11356-022-20808-8

RESEARCH ARTICLE

Effect of ventilation quantity on electron transfer capacity and spectral characteristics of humic substances during sludge composting

Zhihan Tan[1,2] · Hongxiang Zhu[3] · Xiaosong He[4] · Beidou Xi[1,2,4] · Yuxin Tian[1,2] · Xiaojie Sun[1,2] · Hongxia Zhang[1,2] · Quanyi Ouche[1,2]

Received: 13 January 2022 / Accepted: 10 May 2022 / Published online: 19 May 2022

Abstract

Humic substances (HSs) can ameliorate soil pollution by mediating electron transfer between microorganisms and contaminants. This capability depends on the redox-active functional structure and electron transfer capacity (ETC) of HS. This study mainly aimed to analyze the effects of different ventilation quantities on the ETC and spectral characteristics of HS (including humic acids (HAs) and fulvic acids (FAs)) during sludge composting. HS was extracted from compost with different ventilation quantities (0.1, 0.2, and 0.3 L kg^{-1} dry matter min^{-1}, denoted as VQ1, VQ2, and VQ3, respectively). The ETC of HS was measured by electrochemical method. Excitation–emission matrix (EEM) spectroscopy, ultraviolet and visible (UV–Vis) spectrophotometry, and Fourier transform infrared (FT-IR) spectroscopy were conducted to understand the evolution of HS composition during composting. Results indicated that the ETC of HA and FA increased during composting, and VQ2 had stronger ETC and electron recycling rate than VQ1 and VQ3 at the end of composting. UV–Vis analysis revealed that the humification degree, aromatization degree, and molecular weight of HA and FA increased during composting, while the content of lignin decreased. EEM-PARAFAC results suggested that VQ2 accelerated the degradation of protein-like substances. FT-IR revealed a decrease trend in polysaccharide and aliphatic, and the carboxyl content increased in VQ2 and VQ3 while decreased in VQ1. Correlation analysis was used to study the relationship between HS components and ETC. The results advance our further understanding of the pollution remediation mechanism of HS.

Keywords Municipal sludge · Aerobic composting · Humic acids · Fulvic acids · UV–visible spectroscopy · Excitation–emission matrix parallel factor analysis

Introduction

Composting is an effective method to treat organic solid waste (Chen et al. 2020a). Compost products play an important role in promoting plant growth, improving soil properties, and enhancing soil carbon sequestration (Jurado et al. 2015; Piccolo et al. 2004; Said-Pullicino et al. 2007). These products also have great potential in remediation of soil pollution (Madejón et al. 2016; Yuan et al. 2016).

Humic substances (HSs) are a complex macromolecular organic matter, including humic acid (HA), fulvic acid (FA), and humin (Guo et al. 2019). HS has electron transfer capacity (ETC) because it has a large number of functional groups with redox activity. HS can transfer electrons between microorganisms and terminal electron receptors as electron shuttles, which mediates the passivation of heavy metals and the degradation of refractory organic pollutants; thus, HS plays an important role in environmental pollution

Responsible Editor: Ta Yeong Wu

✉ Xiaojie Sun
sunxiaojie@glut.edu.cn

[1] Guangxi Key Laboratory of Environmental Pollution Control Theory and Technology, Guilin University of Technology, Guilin 541004, China

[2] Guangxi Collaborative Innovation Center for Water Pollution Control and Water Safety in Karst Area, Guilin University of Technology, Guilin 541004, China

[3] College of Light Industry and Food Engineering, Guangxi University, Nanning 530004, China

[4] State Environmental Protection Key Laboratory of Simulation and Control of Groundwater Pollution, Chinese Research Academy of Environmental Sciences, Beijing 100012, China

remediation (Wu et al. 2017). Examples of this method are reduction of Cr(VI) to Cr(III) (Yang et al. 2020), reduction of Fe(III) to Fe(II) (Stern et al. 2018), reduction of nitrobenzene to aniline (Yuan et al. 2017), and reduction and dechlorination of pentachlorophenol (Zhao et al. 2020). HS also has the characteristic of transferring electrons repeatedly and can further accelerate the transformation rate of pollutants (Xu et al. 2009). Electron recycling rate (ERR) is often used to measure the durative of electron transfer (Yuan et al. 2012). The application of compost in soil remediation actually depends on the ETC and ERR of HS in compost. The value of compost in soil remediation is higher when the ETC and ERR values are stronger (Zhang et al. 2021a). Therefore, ETC and ERR of HS are important indicators to determine its environmental effect (Azim et al. 2018).

Ventilation quantity is an important parameter that affects composting process (Gao et al. 2010). Insufficient ventilation can cause anaerobic phenomenon, but excessive ventilation can decrease the compost temperature and may not be conducive to the degradation of organic matter (Ahn et al. 2007). The heat and temperature of the piles can be adjusted by regulating the ventilation volume; thus, the degradation of organic matter and the formation of HS are affected (Chen et al. 2020b). Most current studies on ventilation quantity focus on the effect of ventilation quantity on physicochemical properties, such as maintaining the temperature of compost, accelerating the degradation of organic matter, and improving germination index (GI) (Zang et al. 2016). However, few studies focus on the effect of ventilation quantity on the composition evolution and ETC of HS, and the change in redox properties of HS during composting with different ventilation quantities is unclear.

The main objectives of this study were as follows. (1) The evolution of ETC during composting with different ventilation quantities was investigated by electrochemical method. (2) The changes in organic composition and structure during composting with different ventilation quantities were analyzed using spectral analysis method to clarify the key affecting factors of ETC of HS. The results provide scientific basis for the application of compost products and the improvement in pollution remediation efficiency of compost products.

Materials and methods

Composting process, sample collection and physical–chemical analysis

The municipal sludges in this study were from a sewage treatment plant in Guilin, China. The sludge and rice bran were evenly mixed at 3:1 (m/m) ratio and then placed into three identical reactors (a total effective volume of approximately 50 L, Φ37× 57 cm) for the continuous aeration composting. The physico–chemical properties of the raw materials are presented in Table 1.

The aeration quantities of the three piles were set as 0.1, 0.2, and 0.3 L kg^{-1} dry matter min^{-1}, which were denoted as VQ1, VQ2, and VQ3, respectively. Each pile was turned over once a week. An electronic thermometer was used to monitor daily temperature during composting. Moisture content (MC) was determined by drying at 105 °C for 4 h, and volatile solid (VS) content was measured by combustion at 650 °C for 6 h. GI was measured with the method provided by Wu et al. 2019.

Samples were collected on days 0, 3, 6, 9, 12, 15, 21, 30, and 40. One part of the samples was stored directly in a −20 °C freezer, and the other part was freeze-dried and passed through a 60-mesh sieve. After screening, the samples were stored in the −20 °C freezer for further analysis.

Extraction and separation of HA and FA

The extraction and evaluation methods of HS refer to the methods of Song et al. (2015) and Zhou et al. (2014). The initial extraction of HS was by lye extraction. The extracted lye was 0.1 mol/L $Na_2P_2O_7$ and 0.1 mol/L NaOH mixed in 1:1 solution, and then, it was placed into the horizontal constant temperature oscillator to oscillate for 24 h. The mixture was centrifuged at 10,000 rpm for 20 min, and the centrifuged supernatant was filtered through a 0.45-μm filtration membrane. The precipitate obtained after centrifugation (4000 rpm for 15 min) was crude HA, and the supernatant was crude FA after the pH of the filtrate was adjusted to 1–2.

The HA was redissolved with 0.1 mol/L NaOH, supernatant was collected after centrifugation (10,000 rpm for 20 min), and pH of supernatant was adjusted to 1–2 with 6 mol/L HCl, followed by static settlement for 6 h. It was centrifugated again, and the supernatant was discarded. Pure HA was obtained after four times washing with distilled water and 0.1 mol/L HCl. The crude FA was passed through the XAD-8 resin column, and the FA was trapped in the resin and then eluted in the resin column with 0.1 mol/L NaOH. The solution was passed into IR120 hydrogen cation exchange resin column to eliminate the interference of sodium ion. Purified

Table 1 The initial properties of raw materials

Parameters	MC (%)	pH	VS (%)	GI (%)
Municipal sludges	83.1 ± 1.1	7.1 ± 0.3	48.48 ±1.2	40.22 ± 5.4
Rice bran	7.5 ±0.7	5.2 ± 0.3	64.14 ±1.5	54.79 ± 3.3

FA was obtained after being freeze-dried. HA and FA were stored in a 4 °C refrigerator for further analysis (Ma et al. 2001).

Electrochemical measurements

The ETC includes electron accepting capacity (EAC) and electron donating capacity (EDC), both of which can be measured by electrochemical methods (Bi et al. 2013). Electrochemical measurements were performed on an electrochemistry workstation CHI660 (Chenhua Co., Ltd., Shanghai, China). The electrochemical detection method uses a three-electrode electrolytic cell device with working electrode (glassy carbon electrode), opposite electrode (platinum column electrode), and reference electrode (Ag/AgCl electrode) (Tang et al. 2019). The purified HA and FA were determined by voltammetry, and 2 g/L ABTS and 2 g/L DQ were used as mediators for oxidation and reduction, respectively (Bi et al. 2013). During the detection, the electrolytic device should be installed first, 2 mL neutral phosphate buffer and 2 mL KCl solution should be added to the electrolytic cell, and nitrogen should be used for 5 min to drain oxygen. Nitrogen should also be used during the detection to ensure stable reading of the detection data. The oxidation potential and reduction potential were set at 0.61 and −0.49 V, respectively, for baseline detection. When the baseline was stable, 1 mL of mediating agent was added into the measuring device for further detection (ABTS was added for EDC detection, and DQ was added for EAC detection). After the reaction was stabilized, diluted HA and FA samples were added to keep TOC at 50 mg/L. The ETC was calculated using the following formula:

$$ETC\,(EDC\ \text{or}\ EAC) = \frac{A_P}{\left(e \times N_A \times M_C\right)}.$$

The unit of EAC and EDC was μmol $e^{-}\cdot(g\ C)^{-1}$, A_p was the Coulomb integral of compost organic matter oxidation curve or compost organic matter reduction curve, and the unit of Coulomb was (C), N_A was Avogadro constant (6.02×10^{23} mol^{-1}), e was the charge per unit electron (1.6×10^{-19} C), M_C was the content of carbon in the reaction system (3.5×10^{-4} g), and ETC of compost sample was the sum of EDC and EAC.

ERR refers to the number of electrons that HS can steadily accept and supply as an electron shuttle. ERR is commonly used to represent its detection device. The potential-step method was used to detect HA and FA, and 0.5–1 mL of purified HA and FA were diluted and added into 2 mL DMSO and 1 mL in the electrolyte solution of 1 mmol/L sodium perchlorate. The total TOC was kept at 50 mg/L, the oxidation and reduction potentials were set at 0.61 and −0.49 V, respectively, and the number of cycles was set to 3. The ERR was calculated using the following formula:

$$ERR = \frac{Q_{cycle2} + Q_{cycle3}}{2Q_{cycle1}} \times 100\%.$$

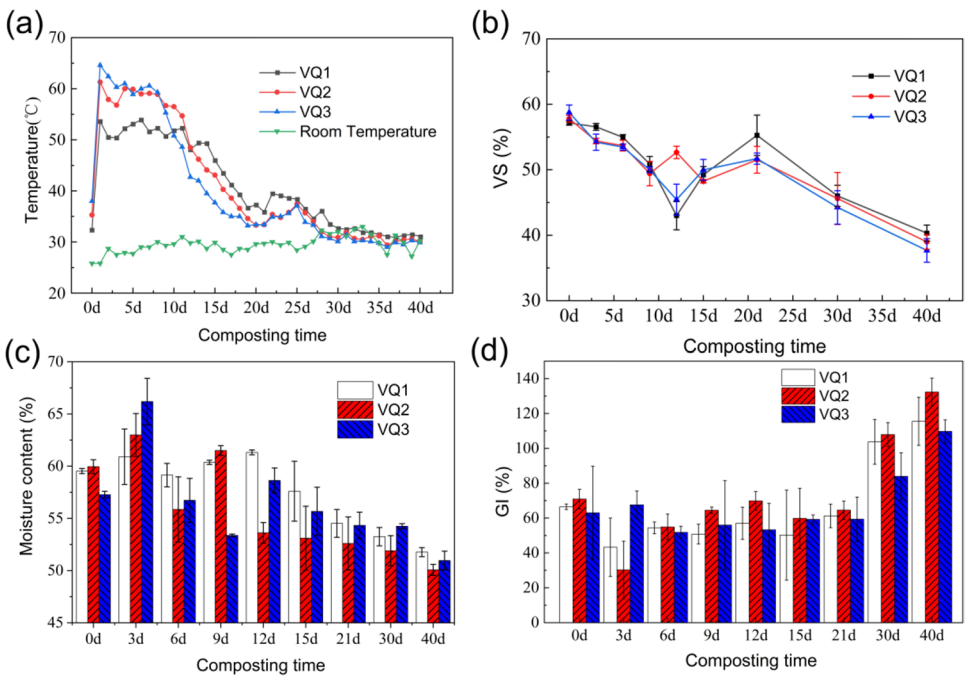

Fig. 1 Changes of physicochemical parameters. Temperature (**a**), VS (**b**), MC (**c**), and GI (**d**) during composting

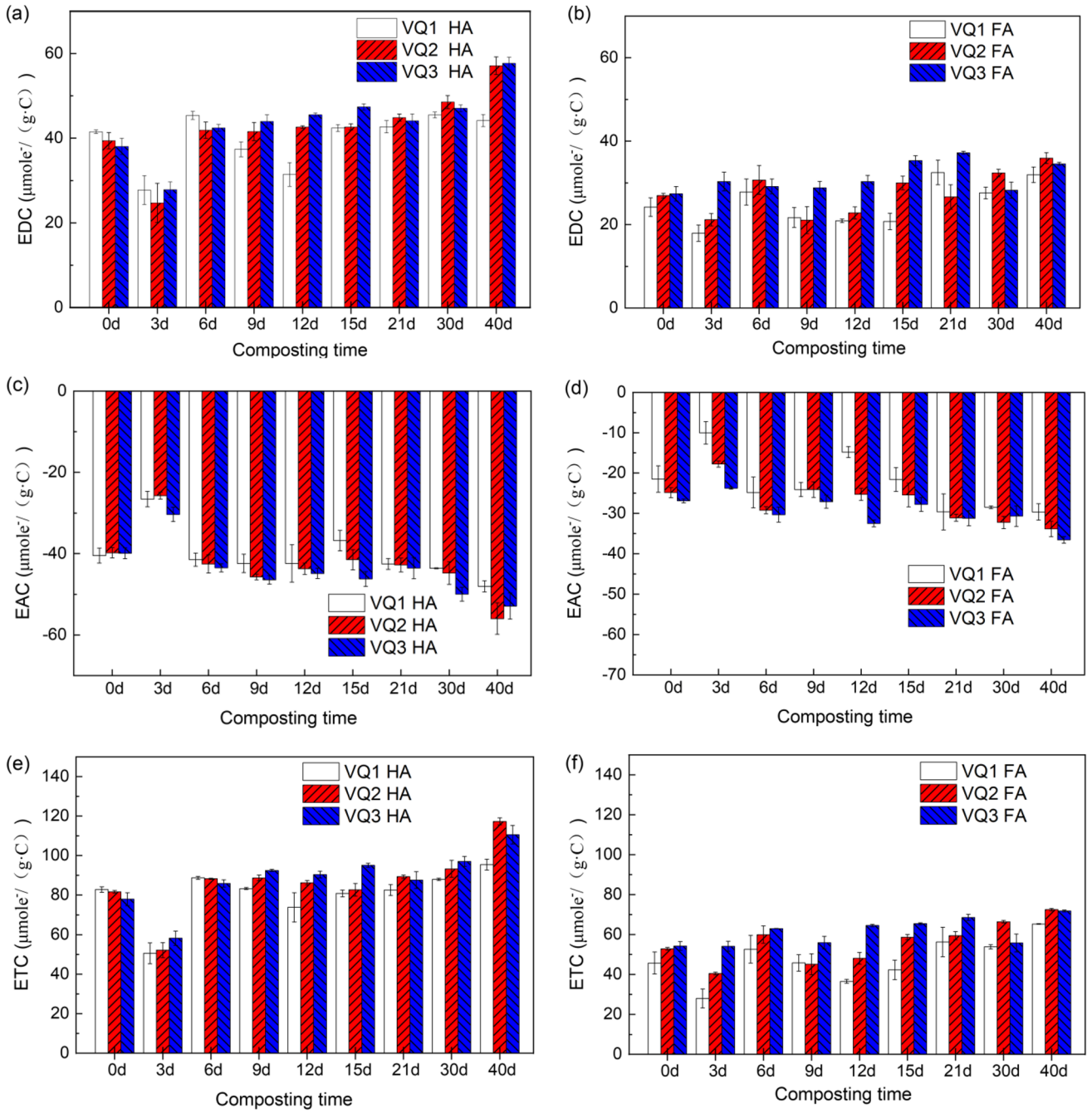

Fig. 2 Changes in EDC (**a**, **b**), EAC (**c**, **d**) and ETC (**e**, **f**) of HA and FA at different stages of compost

Structure and component characterization of organic compounds

Fluorescence spectra

The composition and evolution of HS in composting process are often detected by excitation–emission matrix (EEM) spectroscopy (Marhuenda-Egea et al. 2007). In this study, the EEM fluorescence spectra were recorded by an F98 fluorescence spectrophotometer (Linguang, Shanghai, China). The excitation wavelength (Ex) was set at 200–450 nm, and the emission wavelength (Em) was set at 280–550 nm. Slit broadband was 5 nm. The scanning speed was set at 3000 nm/min.

The fluorescence spectra image of HS was transformed into a matrix, and MATLAB R2018 was used

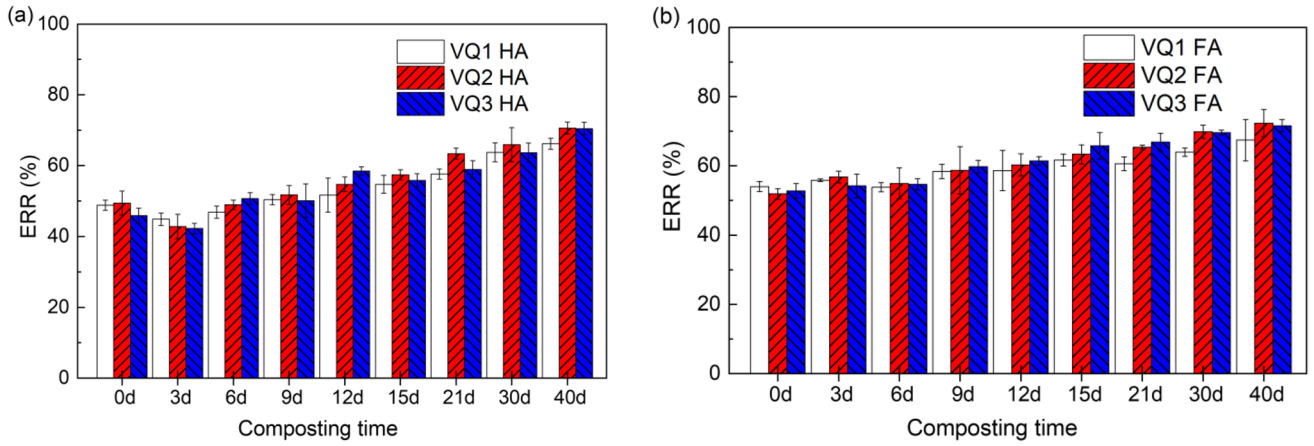

Fig. 3 Changes in ERR of HA (**a**) and FA (**b**) at different stages of compost

for PARAFAC analysis. DOMFluor and EEMscat toolkit (www.models.life.ku.dk) were used to separate the components and calculate the content of each component in the sample. Before separation, the blank sample was deducted to reduce the influence of Raman scattering (Stedmon et al. 2003). Humification index (HIX) and fluorescence index (FI) were calculated by pickpeaks function. HIX was an important index to reflect the humification degree of compost, while FI could reflect the contribution degree of aromatic substances and nonaromatic substances to compost (He et al. 2013; Wang et al. 2016).

Ultraviolet and visible spectrophotometry

Ultraviolet and visible (UV–Vis) spectrophotometry was performed with UV-2820 UV–Vis spectrophotometer (Unique, USA). TOC was diluted to 20 mg/L before scanning, and pure water was used as blank control group. The scanning wavelength ranged from 190 to 700 nm, and the scanning interval was 1 nm.

Fourier transform infrared spectroscopy

Fourier transform infrared spectroscopy (FT-IR) was conducted using an infrared spectrophotometer (Is10, ThermoFisher, USA) for detection. Freeze-dried sample and KBr after grinding were mixed with a mass ratio of 1:100 and then ground with agate mortar. The mixed samples after grinding were placed into a tablet pressing mold for pressing. The pressed glass slides were uniformly transparent and placed into infrared spectrograph to determine the scanning range of 450–4000 cm^{-1}, the number of scanning was set to 14, and the resolution was 2 cm^{-1}.

Results and discussion

Physico–chemical analysis

All treatments reach peak temperature on day 1 (Fig. 1a), and VQ3 has the highest peak temperature possibly due to the higher ventilation quantity. The three treatments last 11, 11, and 10 days in the thermophilic phase (>50 °C), respectively. The temperature of VQ1 during thermophilic stage is significantly lower than that of VQ2 and VQ3, which may be due to the decrease in microbial activity caused by insufficient ventilation. The change in VS could reflect the degradation of organic matter (Fig. 1b). At the end of composting, the VS of three treatments decreases by16.6%, 18.8%, and 21.1%, respectively, which indicates that the increase in ventilation quantity promotes the degradation of organic matter.

The MC of the three treatments increases on days 0–3, and then, it gradually decreases until the end of composting (Fig. 1c). The MC of VQ2 decreases most significantly, which may be related to the longer duration of thermophilic stage. GI is commonly used to evaluate the phytotoxicity and maturity of compost (Yang et al. 2015). The GI of three treatments fluctuates up and down in the range of 30–60% at the early stage of composting (Fig. 1d). After day 30, the GI values of three treatments increase rapidly. Eventually, the GI of VQ2 (132.3%) is higher than that of VQ1 (115.6%) and VQ3 (109.8%). The results show that all three treatments reach maturity (>80%), and the maturity of VQ2 is the highest.

ETC evolution of HS during composting

The ETC of HA and FA samples is shown in Fig. 2. The EDC and EAC of HA show an overall upward

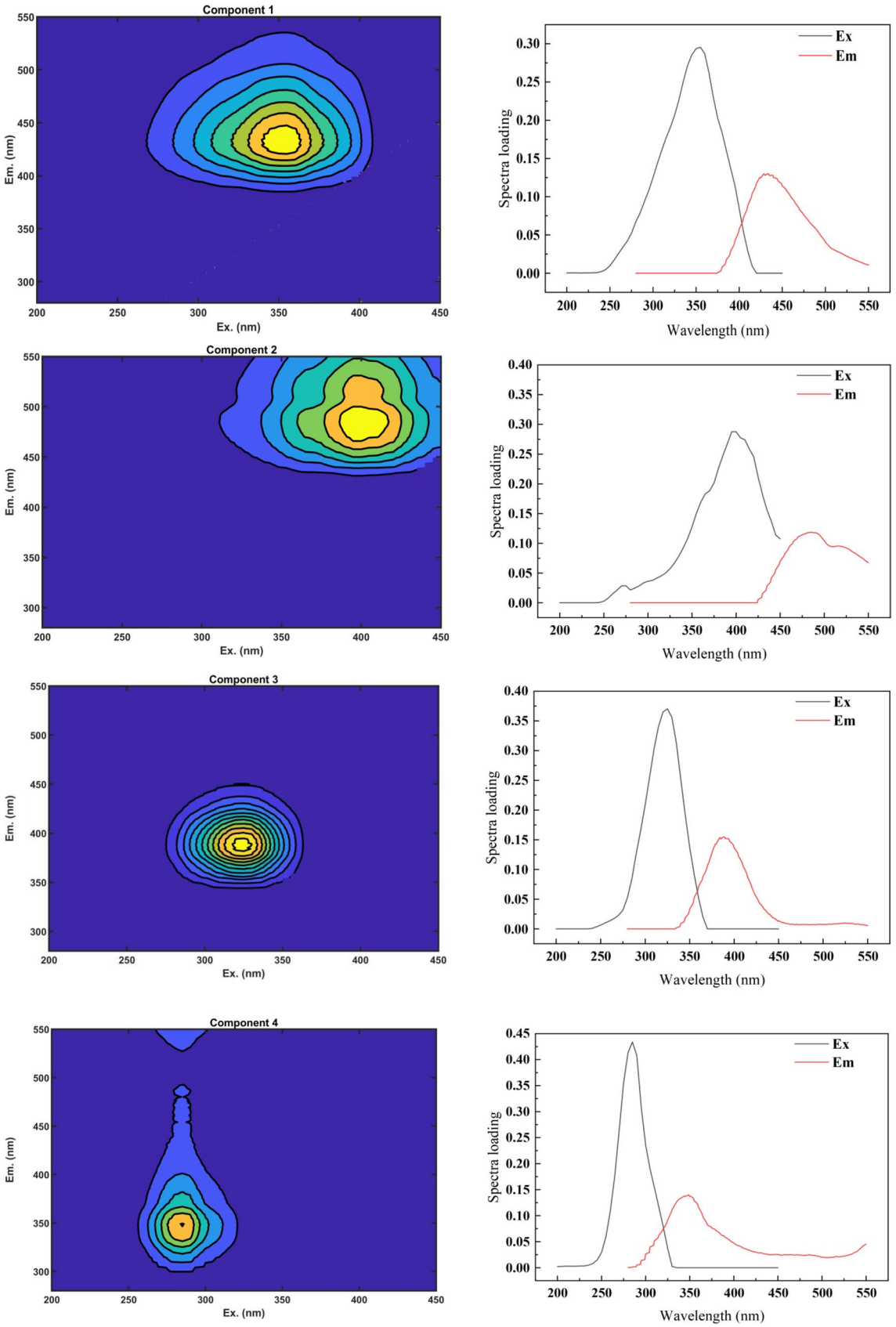

Fig. 4 Overview of each component and related fluorescence load obtained after three-dimensional fluorescence parallel factor analysis

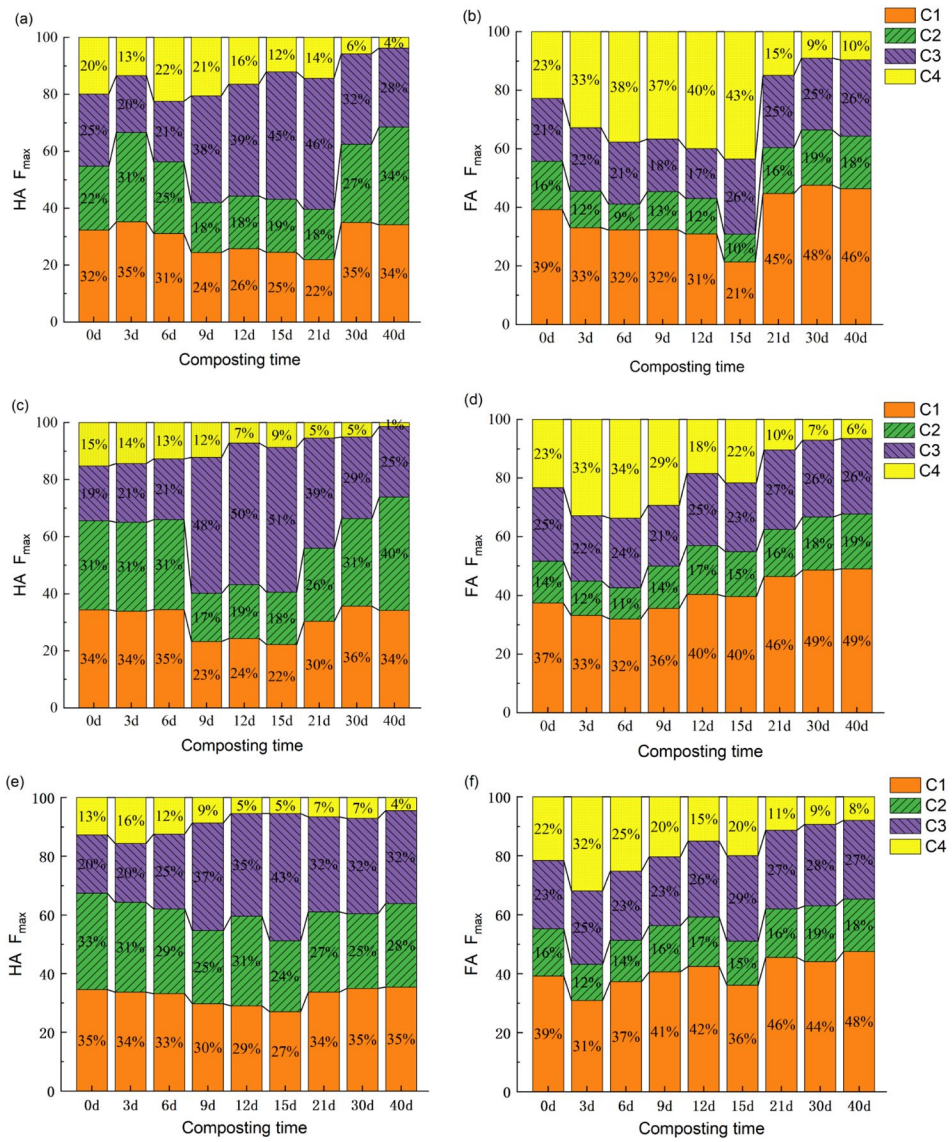

Fig. 5 Changes in the proportion of HA and FA in each stage of compost humic substances. VQ1 (**a**, **b**). VQ2 (**c**, **d**). VQ3 (**e**, **f**)

trend. The EDC of HA of VQ1, VQ2, and VQ3 gradually increases from day 0 (41.52, 39.41, and 38.06 μmol e^-/g C, respectively) to the maximum on day 40 (44.15, 57.12, and 57.66 μmol e^-/g C, respectively); the EAC gradually increases from day 0 (40.45, 39.76, and 39.91 μmol e^-/g C, respectively) to the maximum on day 40 (48.02, 55.96, and 52.90 μmol e^-/g C, respectively). The increase in EDC and EAC may be due to the oxidation of lignin-like matter and the increases in phenols, quinones, and carboxyl groups in HA during composting (He et al. 2019). The increasing trend of the ETC of HA in the three piles is similar to that of EDC and EAC; it reaches the maximum value on the 40th day, and it reaches 92.17, 113.08, and 110.56 μmol e^-/g C for the three piles, respectively. The ETC of HA in VQ2 and VQ3 is stronger than that in VQ1, while the difference between VQ2 and VQ3 is not obvious.

The EDC of FA fluctuates from day 0 (24.22, 26.92, and 27.37 μmol e^-/g C) to day 40 (31.95, 35.34, and 34.56 μmol e^-/g C), which may be due to the degradation of organic matter that increases the reducing group content in FA. EAC increases from day 0 (40.45, 24.83, and 26.68 μmol e^-/g C) to day 40 (48.02, 33.84, and 36.54 μmol e^-/g C), which is similar to EDC. The EAC of FA increases gradually, which is possibly due to the decomposition of protein-like substances and aromatic polycondensation during the composting process (He et al. 2019). The ETC of FA in the three piles shows an increasing trend, and it reaches the maximum value at day 40 (65.3, 72.45, and 71.86 μmol e^-/g C).

In summary, the ETC of FA and HA in VQ2 is stronger than that in VQ1 and VQ3, which may be due to that VQ2 improves the degradation and humification process and promotes the oxidation of organic matter and the formation of HSs. A slight difference is also observed in the

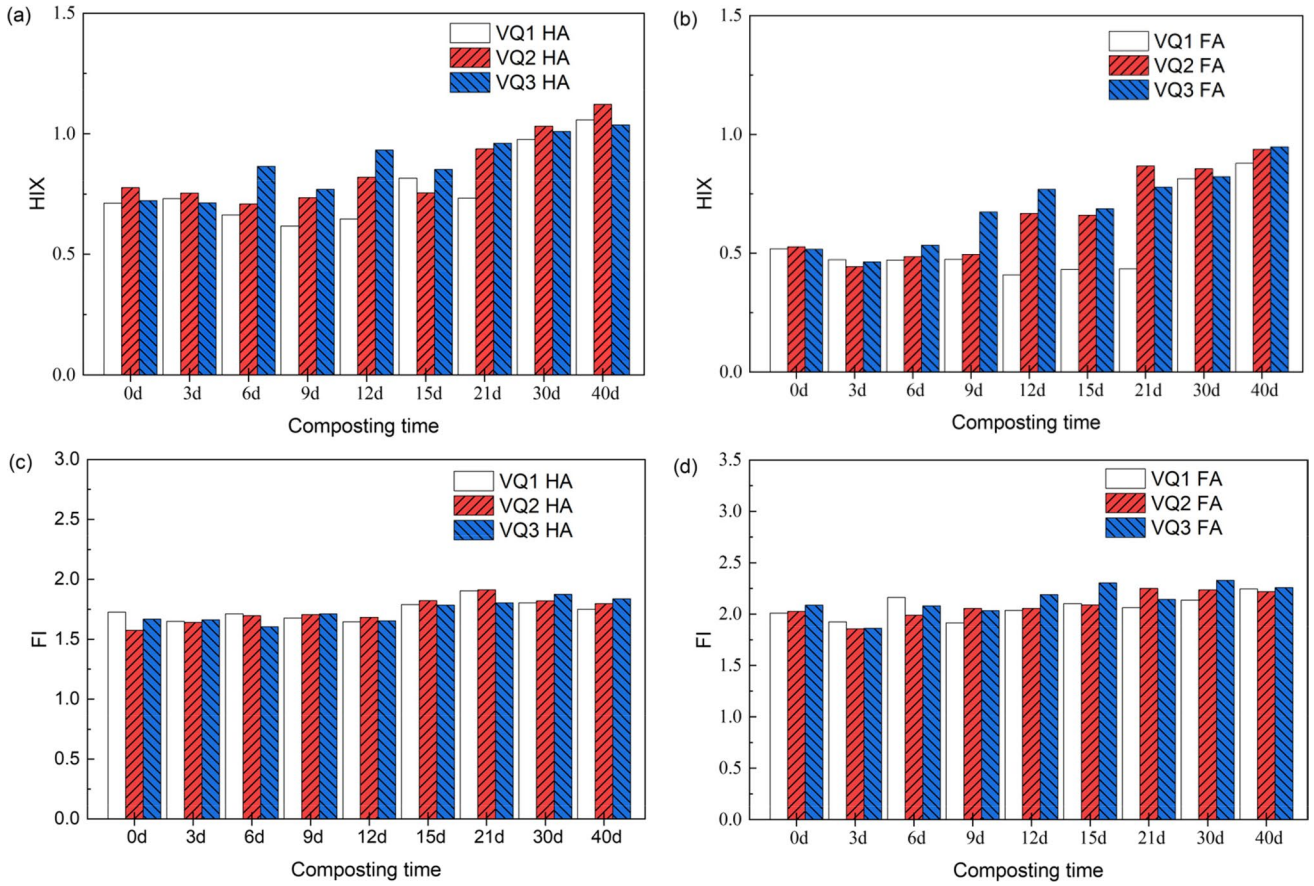

Fig. 6 Changes of HIX index of HA (**a**), FA (**b**) and FI index of HA (**c**), FA (**d**) in compost humic substances

contribution of EAC and EDC to ETC in HA and FA, which indicates that the oxidation and reduction capacities of HS are the same. This result is different from those of the study of He et al. (2014a).

The ERR of HA and FA in the three piles is shown in Fig. 3. HA and FA show a slightly declining trend first and then a rising trend. The ERR of HA is in the range of 45.82–70.59%, and that of FA is in the range of 51.88–72.37%. Only a slight difference is observed between FA and HA in ERR. However, FA has a slightly higher

ERR than HA. This result may be due to the fact that FA contains a large number of unstable electron groups and has a stronger cyclic reaction capacity.

Composition and structure evolution of HS and its influence on ETC

EEM fluorescence spectra

Four components were identified through PARAFAC analysis (Fig. 4). Component 1 (C1, Ex=345 nm, Em=430 nm) shows one excitation peak and one emission peak ascribed to HA peak (Ex=300–370 nm, Em=420–510 nm). The result is similar to the humic-like substance peak discovered by Zhou et al. (2019). Component 2 (C2, Ex=400 nm, Em=485 nm) also shows a single excitation peak and an emission peak located in the humic-like substance peak region, but its Ex has a blue shift. Component 3 (C3, Ex=320 nm, Em=389 nm) peak is located in the traditional fulvic-like region (Ex=310–369 nm, Em=370–450 nm), which corresponds to fulvic-like substances. The peak of component 4 (C4, Ex=240 nm, Em=351 nm) is located in the T-peak region (Ex=270–280 nm, Em=320–350 nm), which mainly reflects protein-like substances such as tryptophan (Zhang et al. 2021b).

HA and FA of the three piles can be divided into four components by PARAFAC analysis, and content changes of different components are shown in Fig. 5. The C4 of the HA decreases gradually with the composting process, which implies that protein-like substances are degraded by microorganisms, and the C4 content in VQ1, VQ2, and VQ3 decreases to 4%, 1%, and 4%, respectively. By contrast, VQ2 has a higher utilization efficiency of organic matter. The content of C4 in FA increases first and then decreases,

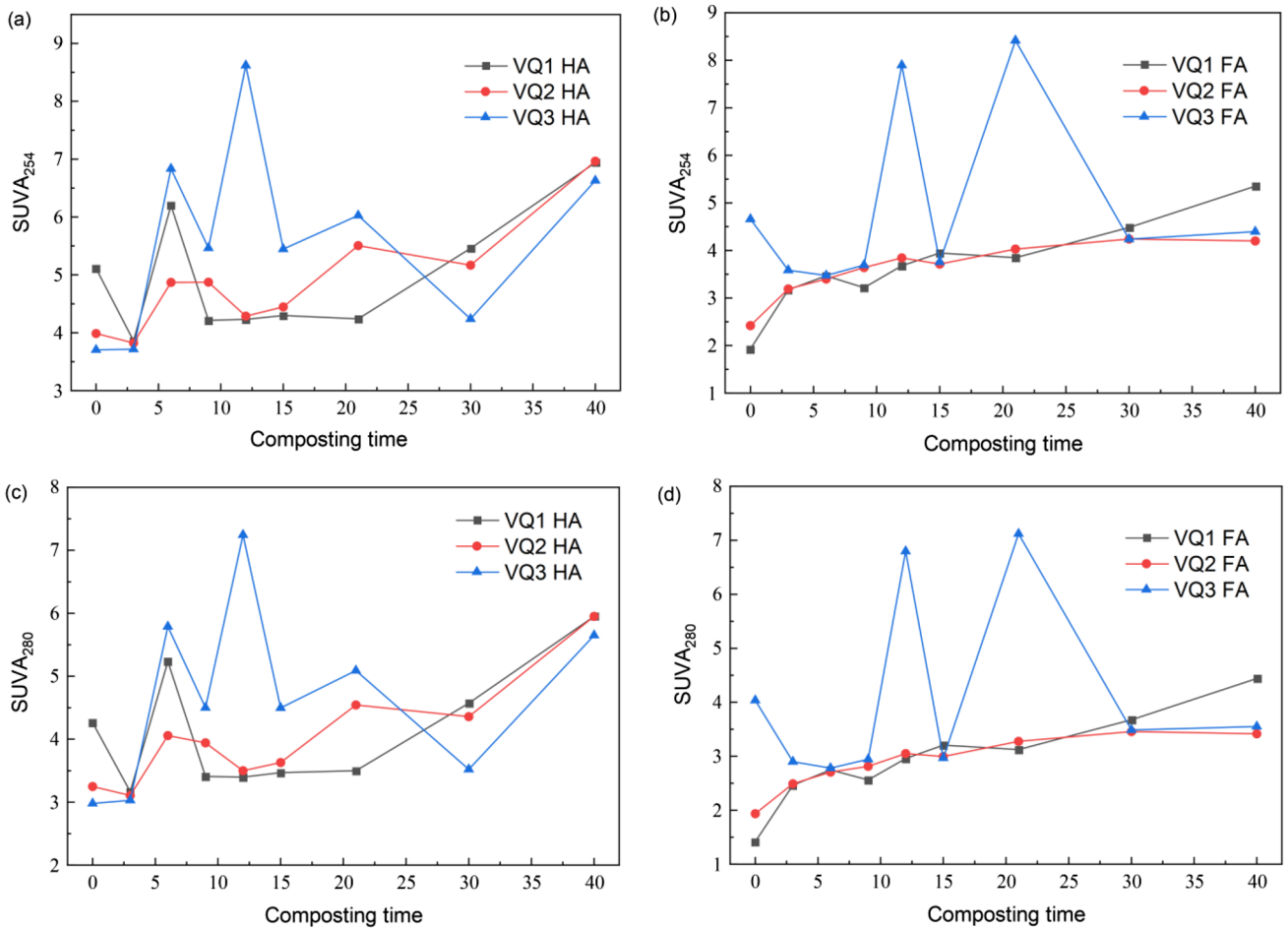

Fig. 7 $SUVA_{254}$ of HA (**a**), FA (**b**) and $SUVA_{280}$ of HA (**c**), FA (**d**) in compost humic substances

but the content of C4 in FA of the three piles decreases to the minimum at the end of composting.

The content of C3 in HA increases first and then decreases, and it increases slightly at the end of composting compared with the initial value. This result may be due to the formation of FA from small molecular substances in composting process. Then, the FA gradually transforms into humic-like substances or HS precursors. However, a slight change is observed in C3 content of FA in the three piles, which may be due to the continuous conversion and degradation of FA (Huang et al. 2021). The content of C2 of HA and FA in the three piles increases, which means the gradual formation of humic-like substances during composting. The C1 of HA at the end of composting is insignificantly different from the initial value, but the C1 of FA shows a significant increase, which is probably due to C1 being closer to the fulvic-like substance in the fluorescence composition. The formation rates of C1, C2, and C3 in VQ2 are the highest, which implies that the degradation of protein and the production of humic-like substances are enhanced in pile VQ2.

The HIX of HA and FA in piles VQ1, VQ2, and VQ3 increases steadily (Fig. 6), and the humification degree of HA is higher than that of FA. Therefore, the composting process increases the humification degree of HA and FA (Jacquin et al. 2017). As shown in Fig. 6, the FI of all three piles gradually increases (McKnight et al. 2001). This result may be due to the microbial degradation and polymerization of organic substances into aromatic structure, such as aromatic groups and benzene ring, which improves the aromatic properties of HA and FA. The FI value of FA is higher than that of HA, which means that aromatic substances in FA contribute more to compost maturity.

UV–Vis spectra

The UV–Vis spectra of HA and FA of the three piles are shown in Fig. S1. The UV–Vis absorption values of the three piles have similar trend, and all of them tend to decrease with the increase in wavelength. HA and FA have an absorption peak at approximately 260–280 band, which is caused by the light absorption of lignosulfonate and its derivatives

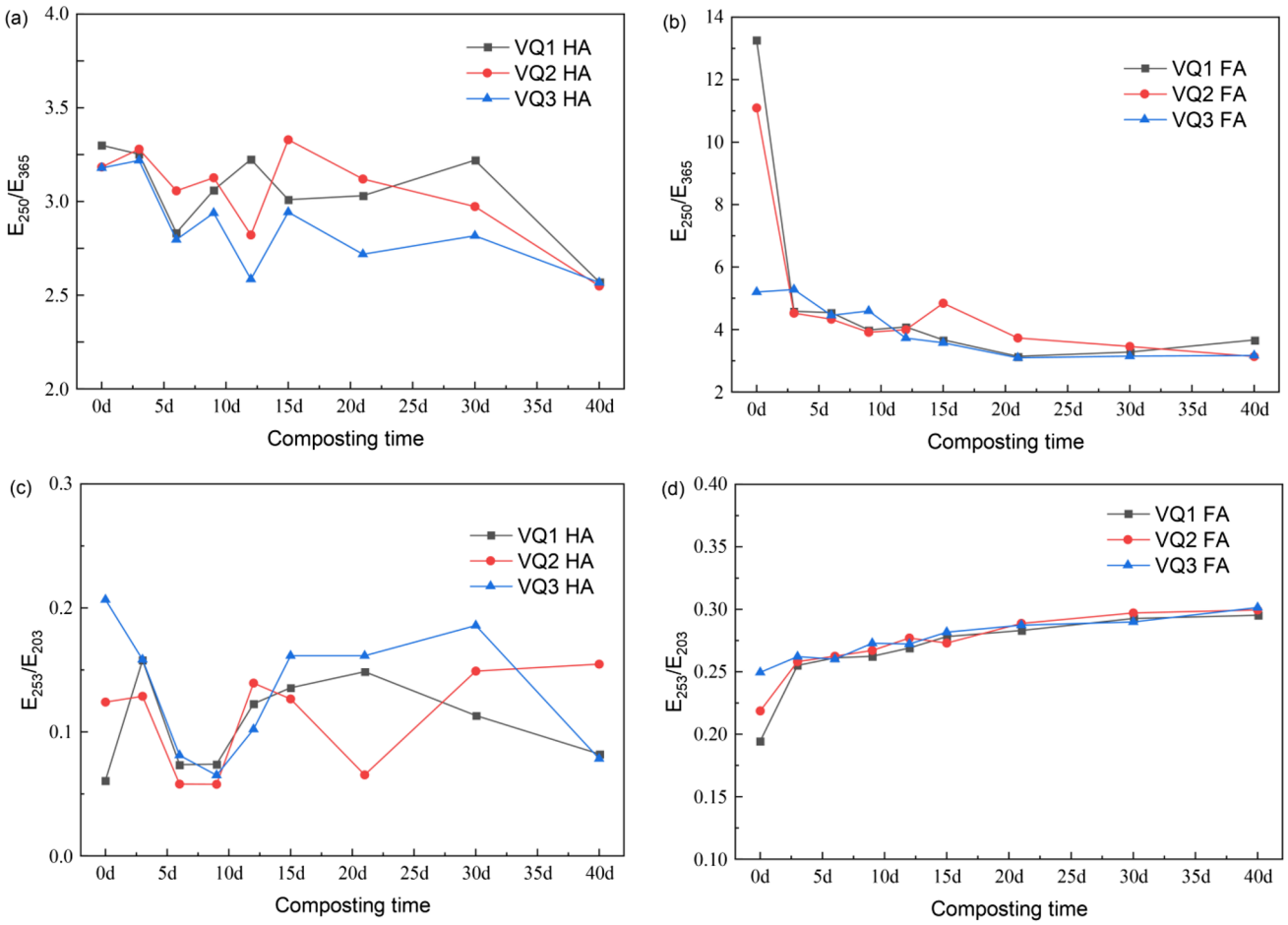

Fig. 8 E_{250}/E_{365} of HA (**a**), Fa (**b**) and E_{253}/E_{203} of HA (**c**), Fa (**d**) in compost humic substances

in the sample, and its absorbance value will increase with the continuous generation of unsaturated conjugated bond C=C/C=O (Li et al. 2010). Except for FA of VQ3, the absorption values of HA and FA at the absorbance of 280 nm increase, which implies that the aromaticity and unsaturation of HS increase, and the degree of humification increases with the progress of composting.

$SUVA_{254}$ and $SUVA_{280}$ (specific ultraviolet absorbance at 254 and 280 nm, respectively) are generally used to represent the content change of unsaturated C=C bond and the change in aromatic molecular weight (Albrecht et al. 2011). During composting, the condensation of lignin and amino acid will increase the HS content, and the absorption value of the $SUVA_{254}$ will also increase (Song et al. 2015). The absorption value of the $SUVA_{280}$ is related to the molecular weight of organic matter (Ren et al. 2019). Both indicators can represent degree of humification. As shown in Fig. 7, $SUVA_{254}$ and $SUVA_{280}$ of HA and FA for VQ1 and VQ2 show an overall increasing trend, which implies that their HS content is increased. The HA of VQ3 shows a fluctuating rise, but its FA shows a fluctuating decline. According to EEM spectrum analysis, this phenomenon may be due to that excessive aeration in the early stage of compost results in a large amount of FA of VQ3, but the unstable structure of FA leads to a low conversion rate in the stable period.

E_{250}/E_{365} is the ratio of lignin to carboxylic acid, and it is often used to indicate the molecular weight of organic matter (Strobel et al. 2001). E_{253}/E_{203} can be used to characterize the types of substituents on the aromatic ring. A lower E_{253}/E_{203} value indicates that the substituents are stable groups such as aliphatic chains, while a higher E_{253}/E_{203} value indicates that the substituents are active groups such as hydroxyl, carboxyl, and carbonyl groups (He et al. 2014b). As shown in Fig. 8, the E_{250}/E_{365} value of HA and FA of the three piles decreases with the composting process. The E_{250}/E_{365} value of HA (2.54–2.56) at the end of composting is lower than that of FA (3.14–3.66), and the decrease in VQ2 is larger, which indicates that more macromolecular HAs are generated in the HS of VQ2 (Said-Pullicino et al. 2007). As shown in Fig. 8, the E_{253}/E_{203} value of HA fluctuates during the composting process, and its increase is most significant in VQ2. Unlike the E_{253}/E_{203} value of HA, that of FA in all

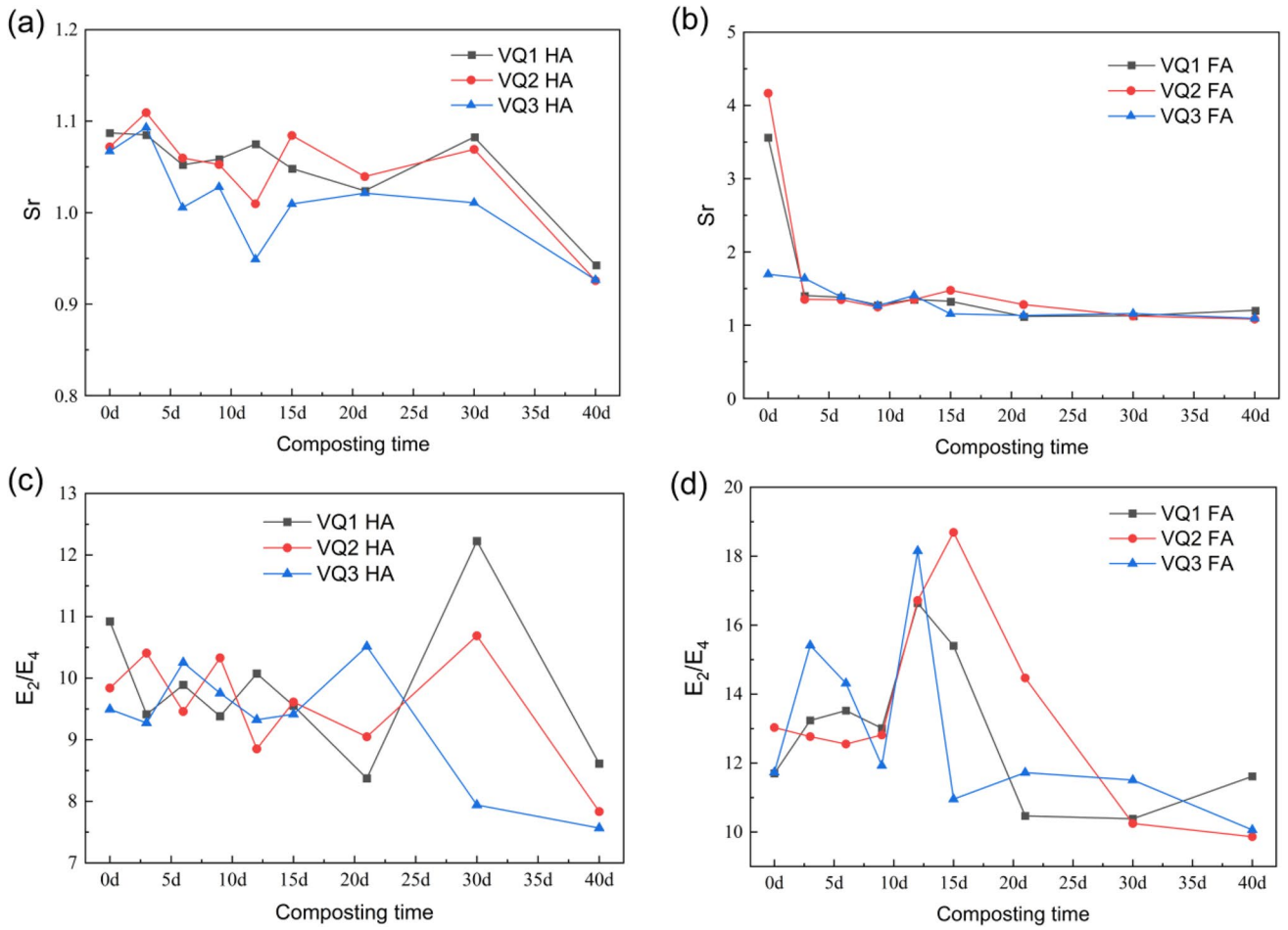

Fig. 9 Sr variation of HA (**a**) and FA (**b**) and E_2/E_4 in compost humic substances

the three piles shows a continuous upward trend. The interaction between HS and heavy metals in soil mainly depends on the transfer of electrons of active groups, and remediation of soil pollution can be achieved through chelating and redox effects of heavy metals (Chen et al. 2019). The change in the E_{253}/E_{203} indicates that soil heavy metals can be better passivated by compost products derived from VQ2.

The ratio of the integral of the 275–295 nm absorption band to the integral of the 350–400 nm absorption band is denoted as Sr, which is negatively correlated with the molecular weight of HS and can be used to characterize the degree of aromatization in HS (Spencer et al. 2012). Fig. 9 a and b show that the Sr value of HA and FA in the three piles decreases continuously with the composting process, which implies that macromolecular aromatic substances increase continuously during composting. E_2/E_4 (= A_{280}/A_{472}) is related to the content of lignin (Biyada et al. 2020). In general, lignin is converted to polyphenols and eventually oxidized to quinone groups and aromatic structures during composting (Che et al. 2020). Fig. 9 c and d show that the E_2/E_4 of HA and FA in the three piles shows a decreasing trend. At the end of composting, the E_2/E_4 values of VQ2 and VQ3 are significantly lower than that of VQ1, which implies that the increase in ventilation quantity promotes the degradation of lignin.

FT-IR results

The FT-IR results of HA and FA of the three piles are shown in Fig. 10. The absorption peaks of HA and FA in the three piles are mainly 3439–3280 cm^{-1}, 2957–2917 cm^{-1}, 2856–2842 cm^{-1}, 1657–1646 cm^{-1}, 1547–1513 cm^{-1}, 1402 cm^{-1}, 1255–1241 cm^{-1}, and 1043–1026 cm^{-1}. The wave peaks of 3439–3280 cm^{-1} in the three piles gradually weaken, which means that O–H functional groups such as hydroxyl group on HA and FA are decreasing during the composting process (Peltre et al. 2017; Soobhany et al. 2017; Sun et al. 2014). The absorption peak of 2957–2917 cm^{-1} may be caused by the C–H antisymmetric vibration of lignin and C–H stretching vibration of aliphatic group (Nasonova et al. 2020). The peak of HA and FA in the three piles weakens and disappears on day 12. Therefore, the fat substances are completely consumed during

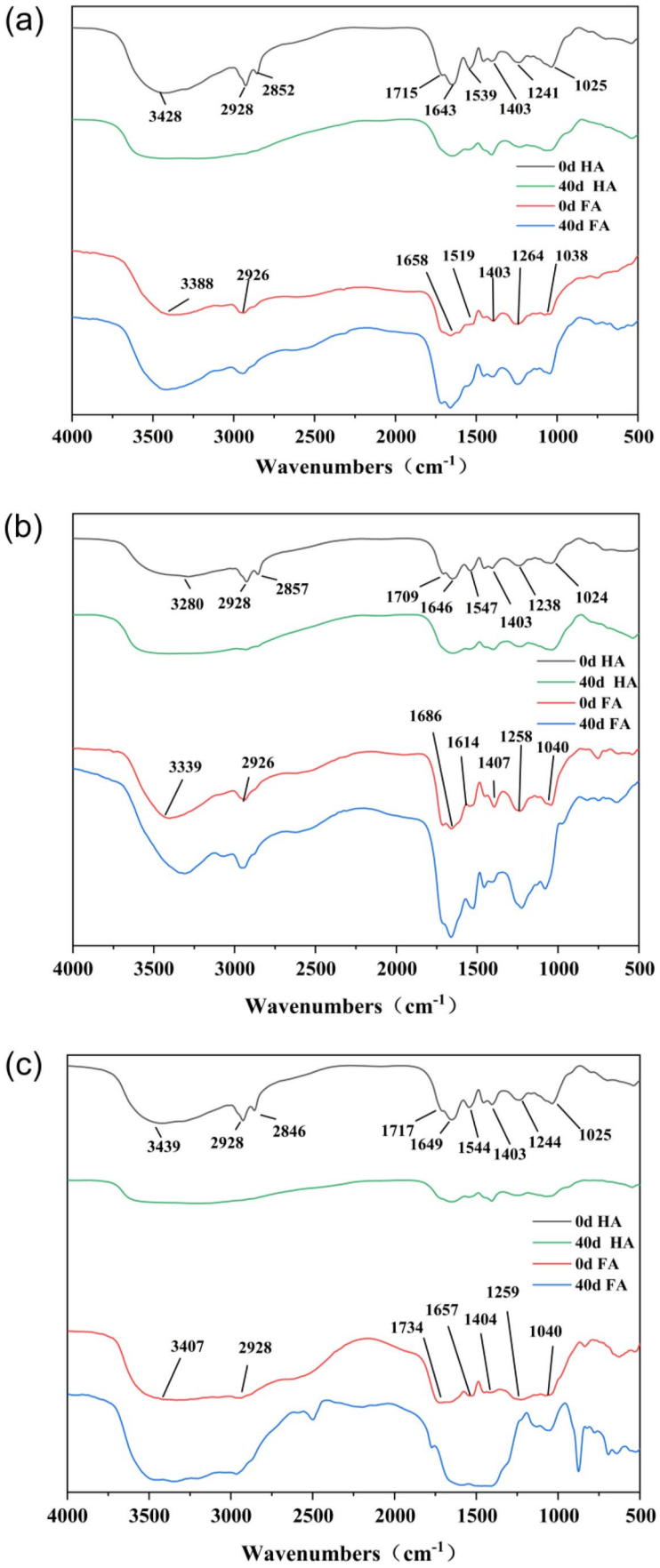

Fig. 10 Infrared spectra of HA and FA of VQ1 (**a**), VQ2 (**b**), and VQ3 (**c**) in compost humic substances

Table 2 The intensity ratios of the major peaks of HA and FA during composting

HA	1646/2928			1646/1403			1646/1025		
	VQ1	VQ2	VQ3	VQ1	VQ2	VQ3	VQ1	VQ2	VQ3
0d	1.010	0.914	0.977	1.840	1.436	1.493	1.597	0.851	1.599
40d	1.246	1.423	1.086	1.949	1.128	1.044	2.082	1.141	1.706
FA	1646/2928			1646/1403			1646/1040		
	VQ1	VQ2	VQ3	VQ1	VQ2	VQ3	VQ1	VQ2	VQ3
0d	1.485	1.835	1.071	1.285	1.599	1.209	1.460	1.621	1.163
40d	1.816	1.953	1.232	1.581	0.741	0.935	1.828	1.937	2.397

the cooling period of compost. The wave peak of 1657–1646 cm^{-1} is the C=C stretching vibration of aromatic group, and the growth degree of VQ2 and VQ3 in this section is higher than that of VQ1, which proves a higher degree for the humification (Masmoudi et al. 2013). The absorption peak of 1547–1513 cm^{-1} may be generated by N–H and C=N stretching vibration, and FA in the VQ2 and VQ3 performs more significant in this section, and HA performs more significant in VQ2 (Merlo et al. 2020). The peak of 1402 cm^{-1} may be caused by the stretching vibration of carboxylic acids, and VQ1 and VQ3 are stronger than VQ2 at 1255–1241 cm^{-1}, which may be caused by the stretching of lignin-related functional groups. The HA and FA of the three piles have little difference at 1043–1026 cm^{-1}, which may be generated by C–O stretching vibration of polysaccharides or alcohols. The analysis of the wave peak above shows that VQ2 has a higher degree of humification.

The changes in the ratios between peaks can further reflect the structural changes of organic matter (Table 2). The ratios of 1646/2928 (aromatic C/aliphatic C) and 1650/1025 (aromatic C/polysaccharides C) both show an increasing trend, which means that aliphatic groups and polysaccharide are degraded, while the aromatic compounds increase during composting. The 1646/1403 (aromatic C/carboxyl C) of VQ1 decreases during composting while that of VQ2 and VQ3 increases, which may be due to the continuous formation of carboxyl C during composting, while the lower ventilation quantity may result in the release of carboxyl C into the environment as CO_2 (Xu et al. 2019).

Relationship among ETC, fluorescence characteristics, and maturity degree of HA and FA in compost with different ventilation quantities

Correlation analysis was conducted to elucidate the relationship among ETC, ERR, maturity degree, and fluorescence characteristics of HA and FA. As shown in Fig. S2, components in HA of VQ1 are insignificantly correlated with changes in EDC, EAC, and ETC. Meanwhile, ERR and C4 are significantly negatively correlated. This result may be due to that the decomposition of protein-like substances will make HS generate more active reversible groups (Amir et al. 2010). HIX is significantly positively correlated with ERR and negatively correlated with C4. Therefore, the decomposition of protein-like substances would increase the degree of humification and improve ERR of HS. FI, Sr, and HIX for FA in VQ1 are significantly positively correlated with EDC, ETC, and ERR, respectively, which indicates that the formation of macromolecular aromatic compounds and the increase in humification degree facilitate improvements in the redox capacity of HS. In VQ2 and VQ3, Sr is positively correlated with EAC in HA, while HIX is positively correlated with EDC, which suggests that humification can improve the redox capacity of HA. C1, C3, and HIX are positively correlated with ETC in VQ2 FA, while they have no obvious correlation in VQ1 and VQ3. Therefore, the formation of humic-like and fulvic-like substances in VQ2 can promote the improvement in ETC of FA. Accordingly, the correlation heat map of VQ3 is similar to that of VQ2, which also proves that C1 and HIX correlate well with the electrochemical indicators.

Conclusion

Physico–chemical parameters show that VQ2 has higher maturity. Spectroscopy analysis shows that the humification degree, aromatization degree, and molecular weight of HA and FA increase during composting with different ventilation quantities, while the content of lignin, polysaccharide, and aliphatic decreases. Electrochemical measurement results reveal that HA and FA in VQ2 have stronger ETC and ERR than those in VQ1 and VQ3 at the end of composting. This finding may due to that VQ2 accelerates the degradation of protein-like substances and improves the humification degree of compost, which enhances the redox capacity of HS.

Supplementary Information The online version contains supplementary material available at https://doi.org/10.1007/s11356-022-20808-8.

Author contribution All authors contributed to the study conception and design. The first draft of the manuscript was written by Zhihan Tan. Material preparation, data collection, and analysis were performed by Quanyi Ouche and Yuxin Tian. Hongxiang Zhu, Xiaosong He, Beidou Xi, Xiaojie Sun, and Hongxia Zhang reviewed and edited the manuscript; all authors commented on previous versions of the manuscript. All authors read and approved the final manuscript.

Funding This work was financially supported by Natural Science Foundation of Guangxi (No. 2018GXNSFGA281001); Science and Technology Major Project of Guangxi (No. AA18118013); and Guangxi Science and Technology Project (No. AD18126018).

Data availability and materials

The datasets used or analyzed during the current study are available from the corresponding author on reasonable request.

Declarations

Ethics approval and consent to participate Not applicable.

Consent for publication Not applicable.

Competing interests The authors declare no competing interests.

References

Ahn HK, Richard TL, Choi HL (2007) Mass and thermal balance during composting of a poultry manure—wood shavings mixture at different aeration rates. Process Biochem 42:215–223

Albrecht R, Le Petit J, Terrom G, Périssol C (2011) Comparison between UV spectroscopy and nirs to assess humification process during sewage sludge and green wastes co-composting. Bioresour Technol 102:4495–4500. https://doi.org/10.1016/j.biortech.2010.12.053

Amir S, Jouraiphy A, Meddich A, El Gharous M, Winterton P, Hafidi M (2010) Structural study of humic acids during composting of activated sludge-green waste: elemental analysis, FTIR and 13C NMR. J Hazard Mater 177:524–529. https://doi.org/10.1016/j.jhazmat.2009.12.064

Azim K, Soudi B, Boukhari S, Perissol C, Roussos S, Alami IT (2018) Composting parameters and compost quality: a literature review. Org Agric 8:141–158

Bi R, Lu Q, Yu W, Yuan Y, Zhou S (2013) Electron transfer capacity of soil dissolved organic matter and its potential impact on soil respiration. J Soils Sediments 13:1553–1560

Biyada S, Merzouki M, Elkarrach K, Benlemlih M (2020) Spectroscopic characterization of organic matter transformation during composting of textile solid waste using UV–visible spectroscopy, infrared spectroscopy and X-ray diffraction (XRD). Microchem J 159:105314. https://doi.org/10.1016/j.microc.2020.105314

Che J, Lin W, Ye J, Liao H, Yu Z, Lin H, Zhou S (2020) Insights into compositional changes of dissolved organic matter during a full-scale vermicomposting of cow dung by combined spectroscopic and electrochemical techniques. Bioresour Technol 301:122757. https://doi.org/10.1016/j.biortech.2020.122757

Chen Y, Chen Y, Li Y, Wu Y, Zeng Z, Xu R, Wang S, Li H, Zhang J (2019) Changes of heavy metal fractions during co-composting of agricultural waste and river sediment with inoculation of Phanerochaete chrysosporium. J Hazard Mater 378:120757. https://doi.org/10.1016/j.jhazmat.2019.120757

Chen T, Zhang S, Yuan Z (2020a) Adoption of solid organic waste composting products: a critical review. J Clean Prod 272:122712. https://doi.org/10.1016/j.jclepro.2020.122712

Chen W, Luo S, Du S, Zhang M, Cheng R, Wu D (2020b) Strategy to strengthen rural domestic waste composting at low temperature: choice of ventilation condition. Waste Biomass Valori 11:6649–6665. https://doi.org/10.1007/s12649-020-00943-4

Gao M, Li B, Yu A, Liang F, Yang L, Sun Y (2010) The effect of aeration rate on forced-aeration composting of chicken manure and sawdust. Bioresour Technol 101:1899–1903. https://doi.org/10.1016/j.biortech.2009.10.027

Guo X, Liu H, Wu S (2019) Humic substances developed during organic waste composting: formation mechanisms, structural properties, and agronomic functions. Sci Total Environ 662:501–510. https://doi.org/10.1016/j.scitotenv.2019.01.137

He X, Xi B, Li X, Pan H, An D, Bai S, Li D, Cui D (2013) Fluorescence excitation–emission matrix spectra coupled with parallel factor and regional integration analysis to characterize organic matter humification. Chemosphere 93:2208–2215. https://doi.org/10.1016/j.chemosphere.2013.04.039

He X, Xi B, Cui D, Liu Y, Tan W, Pan H, Li D (2014a) Influence of chemical and structural evolution of dissolved organic matter on electron transfer capacity during composting. J Hazard Mater 268:256–263. https://doi.org/10.1016/j.jhazmat.2014.01.030

He X, Xi B, Pan H, Li X, Li D, Cui D, Tang W, Yuan Y (2014b) Characterizing the heavy metal-complexing potential of fluorescent water-extractable organic matter from composted municipal solid wastes using fluorescence excitation–emission matrix spectra coupled with parallel factor analysis. Environ Sci Pollut Res 21:7973–7984. https://doi.org/10.1007/s11356-014-2751-9

He X, Yang C, You S, Zhang H, Xi B, Yu M, Liu S (2019) Redox properties of compost-derived organic matter and their association with polarity and molecular weight. Sci Total Environ 665:920–928. https://doi.org/10.1016/j.scitotenv.2019.02.164

Huang W, Li Y, Liu X, Wang W, Wen P, Yu Z, Zhou S (2021) Linking the electron transfer capacity with the compositional characteristics of dissolved organic matter during hyperthermophilic composting. Sci Total Environ 755:142687. https://doi.org/10.1016/j.scitotenv.2020.142687

Jacquin C, Lesage G, Traber J, Pronk W, Heran M (2017) Three-dimensional excitation and emission matrix fluorescence (3DEEM) for quick and pseudo-quantitative determination of protein- and humic-like substances in full-scale membrane bioreactor (MBR). Water Res 118:82–92. https://doi.org/10.1016/j.watres.2017.04.009

Jurado MM, Suárez-Estrella F, López MJ, Vargas-García MC, López-González JA, Moreno J (2015) Enhanced turnover of organic matter fractions by microbial stimulation during lignocellulosic waste composting. Bioresour Technol 186:15–24

Li M, He X, Liu J, Xi B, Zhao Y, Wei Z, Jiang Y, Su J, Hu CM (2010) Study on the characteristic UV absorption parameters of dissolved organic matter extracted from chicken manure during composting. Spectrosc Spectr Anal 30:3081–3085 (in Chinese)

Ma H, Allen HE, Yin Y (2001) Characterization of isolated fractions of dissolved organic matter from natural waters and a wastewater effluent. Water Res 35:985–996. https://doi.org/10.1016/S0043-1354(00)00350-X

Madejón P, Domínguez MT, Díaz MJ, Madejón E (2016) Improving sustainability in the remediation of contaminated soils by the use of compost and energy valorization by Paulownia fortunei. Sci Total Environ 539:401–409. https://doi.org/10.1016/j.scitotenv.2015.09.018

Marhuenda-Egea FC, Martínez-Sabater E, Jordá J, Moral R, Bustamante MA, Paredes C, Pérez-Murcia MD (2007) Dissolved organic matter fractions formed during composting of winery and distillery residues: Evaluation of the process by fluorescence excitation–emission matrix. Chemosphere 68:301–309. https://doi.org/10.1016/j.chemosphere.2006.12.075

Masmoudi S, Jarboui R, El Feki H, Gea T, Medhioub K, Ammar E (2013) Characterization of olive mill wastes composts and their humic acids: stability assessment within different particle size fractions. Environ Technol 34:787–797

McKnight DM, Boyer EW, Westerhoff PK, Doran PT, Kulbe T, Andersen DT (2001) Spectrofluorometric characterization of dissolved organic matter for indication of precursor organic material and aromaticity. Limnol Oceanogr 46:38–48. https://doi.org/10.4319/lo.2001.46.1.0038

Merlo C, Vázquez C, Iriarte AG, Romero CM (2020) Chemical and spectroscopic characterization of humic substances from sediment and riparian soil of a highly polluted urban river (Suquía River, Córdoba, Argentina). Int J Sediment Res 35:287–294. https://doi.org/10.1016/j.ijsrc.2019.10.004

Nasonova A, Levy GJ, Borisover M (2020) Bulk and water-extractable organic matter from compost: evaluation of the selective dissolution in water using infrared absorbance ratios. Environ Sci Pollut Res 27:42644–42655. https://doi.org/10.1007/s11356-020-10153-z

Peltre C, Gregorich EG, Bruun S, Jensen LS, Magid J (2017) Repeated application of organic waste affects soil organic matter composition: evidence from thermal analysis, FTIR-PAS, amino sugars and lignin biomarkers. Soil Biol Biochem 104:117–127. https://doi.org/10.1016/j.soilbio.2016.10.016

Piccolo A, Spaccini R, Nieder R, Richter J (2004) Sequestration of a biologically labile organic carbon in soils by humified organic matter. Clim Chang 67:329–343

Ren X, Wang Q, Awasthi MK, Zhao J, Tu Z, Li R, Wen L, Zhang Z (2019) Effect of tertiary-amine bentonite on carbon transformation and global warming potential during chicken manure composting. J Clean Prod 237:117818. https://doi.org/10.1016/j.jclepro.2019.117818

Said-Pullicino D, Erriquens FG, Gigliotti G (2007) Changes in the chemical characteristics of water-extractable organic matter during composting and their influence on compost stability and maturity. Bioresour Technol 98:1822–1831. https://doi.org/10.1016/j.biortech.2006.06.018

Song C, Li M, Xi B, Wei Z, Zhao Y, Jia X, Qi H, Zhu C (2015) Characterisation of dissolved organic matter extracted from the bio-oxidative phase of co-composting of biogas residues and livestock manure using spectroscopic techniques. Int Biodeterior Biodegradation 103:38–50. https://doi.org/10.1016/j.ibiod.2015.03.032

Soobhany N, Gunasee S, Rago YP, Joyram H, Raghoo P, Mohee R, Garg VK (2017) Spectroscopic, thermogravimetric and structural characterization analyses for comparing municipal solid waste composts and vermicomposts stability and maturity. Bioresour Technol 236:11–19. https://doi.org/10.1016/j.biortech.2017.03.161

Spencer R G, Butler K D, Aiken G R (2012) Dissolved organic carbon and chromophoric dissolved organic matter properties of rivers in the USA. J. Geophys. Res., 117,G03001. https://doi.org/10.1029/2011JG001928

Stedmon CA, Markager S, Bro R (2003) Tracing dissolved organic matter in aquatic environments using a new approach to fluorescence spectroscopy. Mar Chem 82:239–254. https://doi.org/10.1016/S0304-4203(03)00072-0

Stern N, Mejia J, He S, Yang Y, Ginder-Vogel M, Roden EE (2018) Dual role of humic substances as electron donor and shuttle for dissimilatory iron reduction. Environ Sci Technol 52:5691–5699. https://doi.org/10.1021/acs.est.7b06574

Strobel BW, Hansen HCB, Borggaard OK, Andersen MK, Raulund-Rasmussen K (2001) Composition and reactivity of DOC in forest floor soil solutions in relation to tree species and soil type. Biogeochemistry 56:1–26

Sun X, Li G, Xiao A, Shi H, Wang Y, Li Y (2014) Analysis on the impact of composting with different proportions of corn stalks and pig manure on humic acid fractions and IR spectral feature. Spectrosc Spectr Anal 34:2413–2418

Tang J, Wang Y, Zhao W, Ye W, Zhou S (2019) Porous hollow carbon tube derived from kapok fibres as efficient metal-free oxygen reduction catalysts. Sci China Technol Sci 62:1710–1718

Wang Y, Zhang M, Fu J, Li T, Wang J, Fu Y (2016) Insights into the interaction between carbamazepine and natural dissolved organic matter in the Yangtze Estuary using fluorescence excitation–emission matrix spectra coupled with parallel factor analysis. Environ Sci Pollut Res 23:19887–19896. https://doi.org/10.1007/s11356-016-7203-2

Wu J, Zhao Y, Qi H, Zhao X, Yang T, Du Y, Zhang H, Wei Z (2017) Identifying the key factors that affect the formation of humic substance during different materials composting. Bioresour Technol 244:1193–1196. https://doi.org/10.1016/j.biortech.2017.08.100

Wu J, Zhao Y, Yu H, Wei D, Yang T, Wei Z, Lu Q, Zhang X (2019) Effects of aeration rates on the structural changes in humic substance during co-composting of digestates and chicken manure. Sci Total Environ 658:510–520. https://doi.org/10.1016/j.scitotenv.2018.12.198

Xu W, Hu P, Zhou S, Li X, Li Y (2009) Electron shuttling function of dissolved organic matter. Environ Sci 30:2297–2301 (in Chinese)

Xu J, Jiang Z, Li M, Li Q (2019) A compost-derived thermophilic microbial consortium enhances the humification process and alters the microbial diversity during composting. J Environ Manag 243:240–249. https://doi.org/10.1016/j.jenvman.2019.05.008

Yang F, Li G, Shi H, Wang Y (2015) Effects of phosphogypsum and superphosphate on compost maturity and gaseous emissions during kitchen waste composting. Waste Manag 36:70–76. https://doi.org/10.1016/j.wasman.2014.11.012

Yang C, Zheng M, Zhang Y, Xi B, Tian Z, He X (2020) Bioreduction of hexavalent chromium: effect of compost-derived humic acids and hematite. Chin Chem Lett 31:2693–2697. https://doi.org/10.1016/j.cclet.2020.04.001

Yuan Y, Tao Y, Zhou S, Yuan T, Lu Q, He J (2012) Electron transfer capacity as a rapid and simple maturity index for compost. Bioresour Technol 116:428–434. https://doi.org/10.1016/j.biortech.2012.03.114

Yuan Y, Tan W, He X, Xi B, Gao R, Zhang H, Dang Q, Li D (2016) Heterogeneity of the electron exchange capacity of kitchen waste compost-derived humic acids based on fluorescence components. Anal Bioanal Chem 408:7825–7833. https://doi.org/10.1007/s00216-016-9885-1

Yuan Y, Xi B, He X, Tan W, Gao R, Zhang H, Yang C, Zhao X, Huang C, Li D (2017) Compost-derived humic acids as regulators for reductive degradation of nitrobenzene. J Hazard Mater 339:378–384. https://doi.org/10.1016/j.jhazmat.2017.06.047

Zang B, Li S, Michel F, Li G, Luo Y, Zhang D, Li Y (2016) Effects of mix ratio, moisture content and aeration rate on sulfur odor emissions during pig manure composting. Waste Manag 56:498–505. https://doi.org/10.1016/j.wasman.2016.06.026

Zhang C, Xi B, Zhang Q, Zhao Y, Wei Z, Jiang Y, Su J, Hu C (2021a) Application status and prospect of compost in soil remediation and quality improvement. Environ Eng 39: 11. https://doi.org/10.13205/j.hjgc.202109025 (in Chinese)

Zhang Q, Xi B, Yang J, Li S, Li X, Zhao X (2021b) Structural characteristics of fulvic acid composted with different materials. China Environ Sci 41:763–770 (in Chinese)

Zhao X, Tan W, Peng J, Dang Q, Zhang H, Xi B (2020) Biowaste-source-dependent synthetic pathways of redox functional groups within humic acids favoring pentachlorophenol dechlorination in composting process. Environ Int 135:105380

Zhou Y, Selvam A, Wong JWC (2014) Evaluation of humic substances during co-composting of food waste, sawdust and Chinese medicinal herbal residues. Bioresour Technol 168:229–234. https://doi.org/10.1016/j.biortech.2014.05.070

Zhou S, Zhang Y, Huang T, Liu YF, Zhang L, Li G, Yue L, Luo X (2019) Spectral characteristics and sources of dissolved organic matter with different relative molecular weight from rainwater from summer and autumn in thezhoucun reservoir based on UV-Vis and EEMs. Environ Sci 40:172–184 (in Chinese)